

Research Article www.acsami.org

Passive Removal of Highly Wetting Liquids and Ice on Quasi-Liquid **Surfaces**

Lei Zhang, Zongqi Guo, Jyotirmoy Sarma, and Xianming Dai*



Cite This: ACS Appl. Mater. Interfaces 2020, 12, 20084-20095



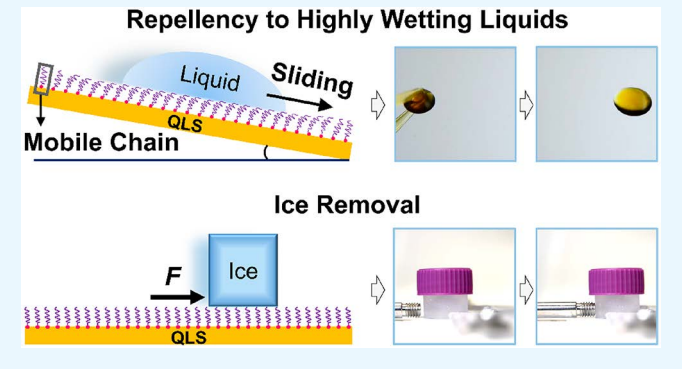
ACCESS I

III Metrics & More

Article Recommendations

Supporting Information

ABSTRACT: Surfaces with ultralow adhesion to liquids and solids have attracted broad interests in both fundamental studies and engineering applications from passive removal of highly wetting liquids and water harvesting to anti-/de-icing. The current state-ofthe-art superomniphobic surfaces (rely on air lubricant) and liquidinfused surfaces (rely on liquid lubricant) suffer from severe issues for liquid repellency and ice removal: air/liquid lubricant loss or topography damage. Here, we create a durable quasi-liquid surface by tethering flexible polymer on various solid substrates. The untethered end of the polymer has mobile chains that behave like a liquid layer and greatly reduce the interfacial adhesion between the surface and foreign liquids/solids. Such a quasi-liquid surface with a 30.1 nm flexible polymer layer shows ultralow contact angle



hysteresis ($\leq 1.0^{\circ}$) to liquids regardless of their surface tensions. The highly wetting perfluorinated liquids like FC72 and Krytox101, as well as complex fluids like urine and crude oil, can be repelled from the surface. Moreover, wind can remove accreted ice from the surface in harsh conditions due to the negligible ice adhesion. We have demonstrated that the quasi-liquid surface shows robust performances in repelling highly wetting liquids, harvesting water, and removing ice, respectively.

KEYWORDS: highly wetting liquids, liquid repellency, water harvesting, ice removal, quasi-liquid surface

■ INTRODUCTION

Surfaces that can passively remove liquids regardless of their surface tensions and ice have attracted broad interests from both interfacial sciences¹⁻⁴ and engineering applications such as fog harvesting, self-cleaning, chemical shielding and anti/ deicing.8 However, passive removal of highly wetting liquids with surface tensions below 18 mN m⁻¹ and accreted ice from the surface remains a challenge.9 Existing passive strategies are centered on either air or liquid lubrication. 2-4,6,7,10 Superomniphobic surfaces (i.e., air lubricated surfaces) use surface topographies to lock air as the lubricant.3,4 When liquid droplets are partially floating on air (i.e., Cassie-Baxter state), 11 the solid-liquid contact areas are dramatically reduced, leading to improved liquid repellency and reduced ice adhesion. However, the air displacement on superomniphobic surfaces results in the transition from the Cassie-Baxter state to the Wenzel state, 12 in which droplets are in full contact with the rough textures. This leads to the failure of liquid repellency and ice removal. Therefore, researchers circumvent the use of air lubricant by creating slippery liquid-infused porous surfaces (SLIPS) (also called liquid-infused surfaces). 13 Such a liquid lubricated surface has molecular smoothness and a mobile interface. Thus, it shows excellent dewetting and anti-icing performances. 14 However, both air lubricant infused superomniphobic surfaces and liquid

lubricant infused slippery surfaces suffer from inherent challenges on durability: lubricant loss and topography damage. For example, air lubricant on superomniphobic surfaces can be displaced in harsh conditions, such as high humidity, 15 large subcooling, 16 turbulent flow, 17 or bioadhesion. 18 Likewise, some types of liquid lubricants on SLIPS evaporate at elevated temperatures, 10 can be displaced by a lubricant-miscible fluid, 19 and may be depleted by the wrapping layer (also called cloaking) on the moving droplets.²⁰ In addition, the surface textures are very likely to be damaged during ice removal.²¹

To achieve a much more desirable nonsticky surface, researchers developed liquid-like surfaces with covalently grafted flexible polymers on flat surfaces, such as slippery omniphobic covalently attached liquid (SOCAL), to form omniphobicity.²²⁻³⁷ Those surfaces are independent of air or liquid lubricant but can still repel organic and aqueous liquids because of the mobile molecular chains tethered on the

Received: February 2, 2020 Accepted: April 7, 2020 Published: April 7, 2020





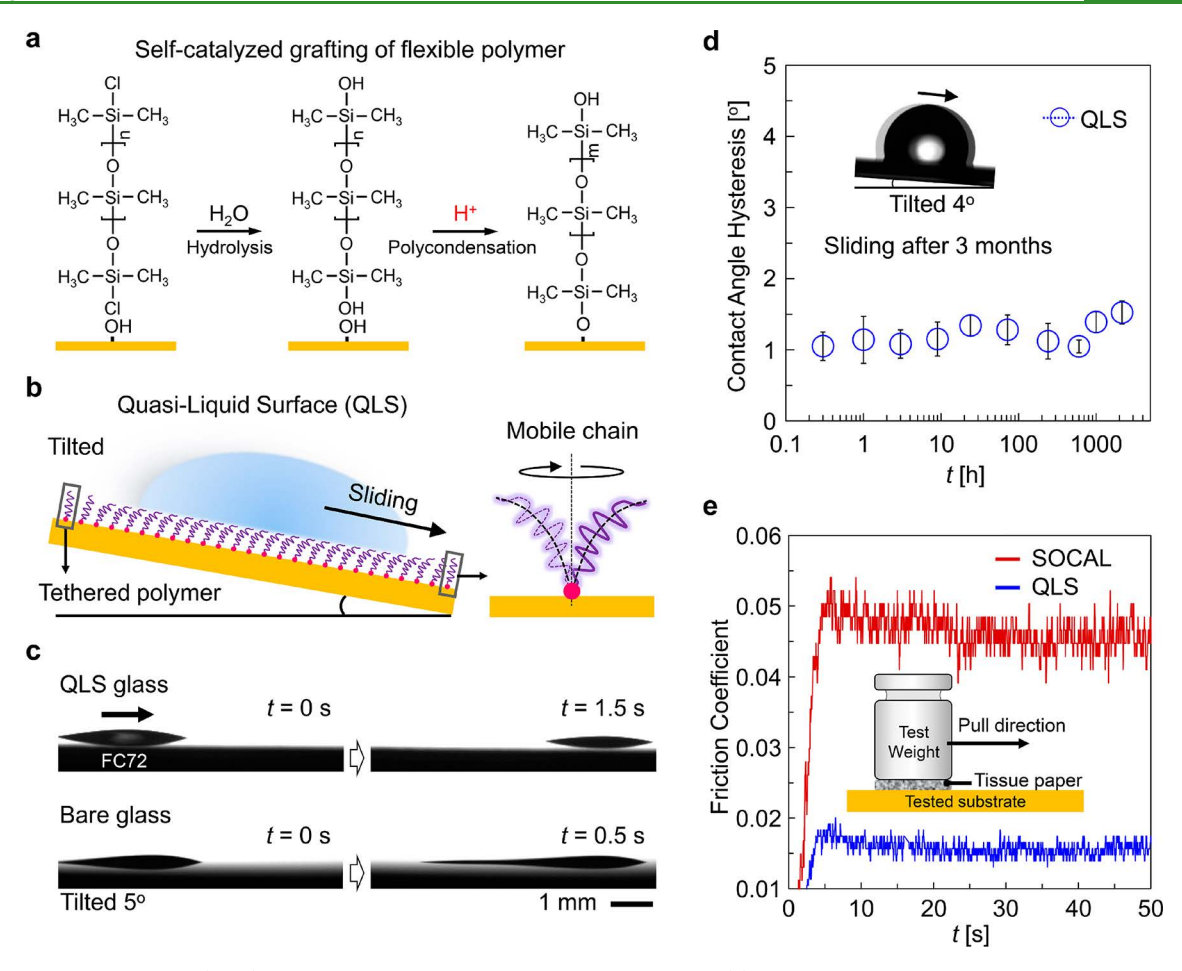


Figure 1. Quasi-liquid surface (QLS) made with flexible polydimethylsiloxane polymer. (a) One-step self-catalyzed grafting of polydimethylsiloxane on a hydroxylated substrate. The number of the repeated units is changed from "n" to "m" due to the growth of the polymer chain. (b) Schematic of droplet sliding on a tilted QLS, where the mobile chain maintains its high mobility through rotational and/or bending motions of the Si–O–Si skeleton. (c) Time-sequence images of liquid repellency of $\sim 2~\mu L$ of FC72 ($\gamma = 10.0~\text{mN m}^{-1}$) on the QLS with a glass substrate and bare glass at a tilted angle of 5°. (d) Water contact angle hysteresis (CAH) as a function of heating time at 105 °C on the QLS with a silicon substrate. The insets show that a 5 μL water droplet can still slide on the QLS after more than 3 months. The CAH values were averaged from at least 5 independent measurements by applying \sim 5 μL droplets on the test platform. (e) The friction coefficient of a load on the QLS and the current state-of-the-art liquid-like surface of SOCAL. A 10.2 kg test weight was used as the load for this measurement.

surfaces. Nevertheless, existing flexible polymer mediated liquid-repellent surfaces still show a few challenges. (i) There is a limit of polymer thickness, which hinders the sustainable removal of liquids and solids. The existing flexible polymer coating uses a small molecule siloxane with a molecular weight of around 400 g/mol as the reactive reagent. 22,29 Therefore, a large number of water molecules are generated and densely adsorbed on the surface during the polycondensation reaction. This severely blocks the growth of the molecular chain.³⁸ In consequence, only a thin polymer coating with a thickness of around 5.0 nm could be grafted on the substrate, leading to the poor antiwearing property, inhomogeneous surface coverage, and defective contact line.²⁷ (ii) The interfacial shear strength of ice on the existing liquid-like surfaces remains unexplored. (iii) Existing grafting methods are not compatible with reactive substrates, as catalysts or organic solvents are often applied in the synthesis process. 24,25,28-30,34,37 Especially, some of the metal surfaces are corroded when the acid catalyst is added in the reaction system, e.g., aluminum.³²

A desired nonsticky surface must be durable, scalable, and robust on various substrates, which can show an ultralow adhesion to a variety of liquids and solids. Here, we report a nonsticky surface that is made by grafting flexible polymers, which have mobile chains on the untethered end and behave like a liquid layer, namely, quasi-liquid surface(s) (QLS(s)). Such a surface has a coating thickness of 30.1 nm that overcomes the thickness limit of the state-of-the-art liquid-like surface (i.e., SOCAL). Although it is reported that liquid repellency is independent of polymer thickness on existing liquid-like surfaces, we elucidate that the polymer thickness is vital for sustainable ice removal. Thus, we show that the QLS addresses the durability challenges in repelling highly wetting liquids during sustainable operations, harvesting water from air, and reducing ice adhesion.

■ RESULTS AND DISCUSSION

Fabrication and Overall Properties of the Quasi-Liquid Surfaces. The quasi-liquid surface is made by tethering one end of the flexible polymer of polydimethylsiloxane on a solid substrate but keeping the other end mobile (Figure 1a). Simultaneous hydrolysis and polycondensation occur in this one-step surface grafting without any solvent, catalyst, or harsh condition. Briefly, chlorine-terminated siloxane is spontaneously hydrolyzed to form hydroxyl-

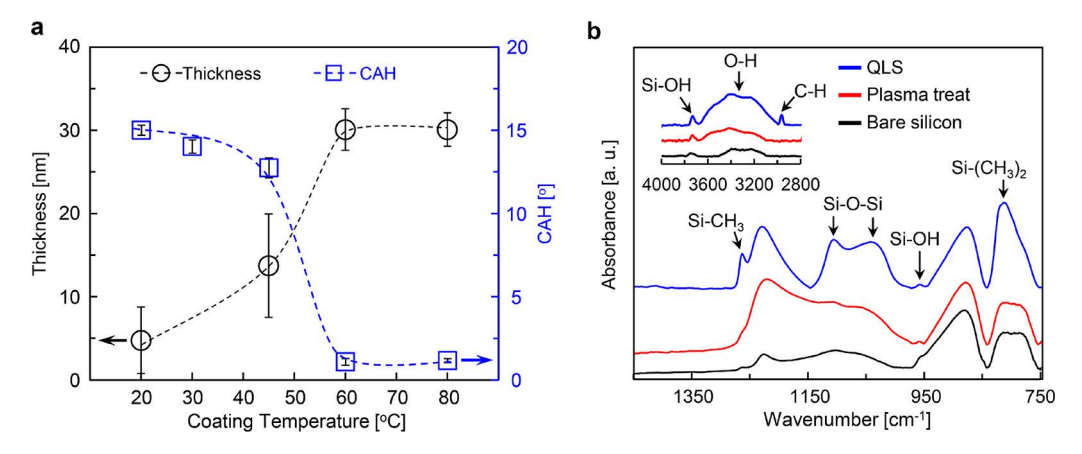


Figure 2. Parametric study of grafting kinetics for the QLS. (a) The influence of the coating temperature on the water CAH on the QLS and the corresponding coating thickness of the QLS measured by an ellipsometer. The average thickness was obtained by 5 independent measurements at different positions on the surface. The CAH values were averaged from at least 5 independent measurements by applying \sim 5 μ L droplets on the test platform. The grafting time was 60 min. All the samples were fabricated by the vapor phase in a vacuum oven. (b) ATR-FTIR spectra of the QLS on silicon (grafting time: 60 min; grafting temperature: 60 °C).

terminated siloxane in the presence of moisture. Then, the covalent grafting and reactive growth of the mobile chain could rapidly proceed via polycondensation, which is self-catalyzed by hydrochloric acid generated from the hydrolysis of chlorineterminated siloxane.³⁹ Herein, we used the siloxane oligomer with a high molecular weight of 2000-4000 g/mol for surface grafting. As a result, the number of byproducts such as water and acid are reduced during the hydrolysis and polycondensation reactions in the grafting process. Reduced water generation enables a long chain to be tethered on the surface.³⁸ The grafted siloxane polymer chain, with one end mobile and the other end tethered, behaves like a quasi-liquid and maintains its high mobility benefiting from its extremely low glass transition temperature ($T_{\rm g}$ = -125 °C) and low rotation barrier of the repeated Si-O-Si bond (bond angle = 143°) (Figure 1b).²³ Although the tethered flexible polymer cannot behave like a real liquid, the unentangled polymer brushes with mobile chains on one end still show liquid-like lubrication in terms of liquid repellency. 40 Its high molecular mobility provides the QLS an unprecedented liquid repellency for both water and organic liquids compared to reported works (Table S1).

In this work, various reaction systems and multiple reaction conditions were studied to obtain the optimized parameter for making QLSs. Either vapor phase or liquid phase reactions could lead to the optimal performance for the QLS (Tables S2 and S3). Unless otherwise specified, all the quasi-liquid surfaces used in this work were made by a vapor phase in a vacuum oven at 60 °C for 60 min (Figure S1). The atomic force microscope (AFM) images show that the QLS has a roughness of 0.35 nm, while the solid coating made of the small molecule silane of chlorotrimethylsilane (Me₃SiCl) and bare glass surface show the roughnesses of 2.26 and 2.72 nm, respectively (Figures S2 and S3). This indicates that the flexible polymer-mediated QLS has an extremely smooth surface. Due to the high light transmission of the polydimethylsiloxane material, QLS shows identical optical transparency compared with a bare glass substrate (Figure S4). QLS can repel liquids regardless of their surface tensions (denoted by γ), such as water ($\gamma = 72.8 \text{ mN m}^{-1}$) and even for the perfluorinated liquids of Krytox101 ($\gamma = 17.0 \text{ mN m}^{-1}$) and FC72 ($\gamma = 10.0 \text{ mN m}^{-1}$) (Figure 1c, Table S4, and

Movies S1 and S2). All the liquid droplets show extremely low contact angle hysteresis (CAH $\Delta\theta \leq 1.0^{\circ}$, Table S4), where the CAH $\Delta\theta$ is the difference between advancing (θ_{adv}) and receding (θ_{rec}) contact angles (i.e., $\Delta\theta = \theta_{adv} - \theta_{rec}$). A small CAH of a liquid droplet indicates a good liquid repellency on the QLS. Furthermore, the QLS is highly thermostable due to the strong bond dissociation energy of Si–O (444 kJ/mol) in the siloxane skeleton and the grafting site on the substrate. ²³ It shows an ultralow CAH ($\Delta\theta \leq 1.5^{\circ}$) for water on the QLS even after heating at 105 °C for more than 3 months (Figure 1d).

Moreover, the QLS shows a much lower adhesion force to the solid than the state-of-the-art liquid-like surface (i.e., SOCAL),³⁷ which can repel liquids with surface tensions from 18.4 to 72.8 mN m⁻¹. The SOCAL exhibits an optimal liquid repellency with a coating thickness of 4.0 nm. However, an increased thickness shows the inhomogeneity of the polymer chains resulting in deteriorated liquid repellency.³⁷ To test the friction coefficient of a solid on the surface, a test load with tissue paper adhered to the bottom was applied to the surface (Figure 1e, inset). Interestingly, the QLS exhibits a static friction coefficient of 0.019, which is 34.5%, 4.5%, and 2.3% of that on the SOCAL (0.055), bare silicon surface (0.42), and cross-linked PDMS (0.83), respectively (Figures 1e and S5). The lower static friction coefficient reveals that QLS with a thicker layer of polymer coating can provide a better interfacial lubrication than SOCAL with a thinner layer.

Parametric Study of Grafting Kinetics for the QLS. To better understand the grafting kinetics, we studied the effects of reaction temperature and reaction time on the mobility of liquid droplets and coating thickness on the QLS. An ellipsometer was used to analyze the thickness of the tethered flexible polymer. As shown in Figure 2a, the CAH and sliding angle (SA) of the water droplets on the QLS show sharp declines when the coating temperature increases to around 50 °C for 60 min. Specifically, the QLS with coating temperatures below 50 °C shows a large CAH ($\Delta\theta > 12^{\circ}$) and SA (>58°) for water. When the coating temperature increases beyond 60 °C, an ultralow water CAH ($\Delta\theta = 1.0^{\circ}$) and SA (4°) are obtained (Figures 2a and S6). The reason is that a thicker and denser polymer layer (thickness = 30.1 nm) can be grafted at 60 °C than that at 20 °C (4.8 nm; Figure 2a). The elevated

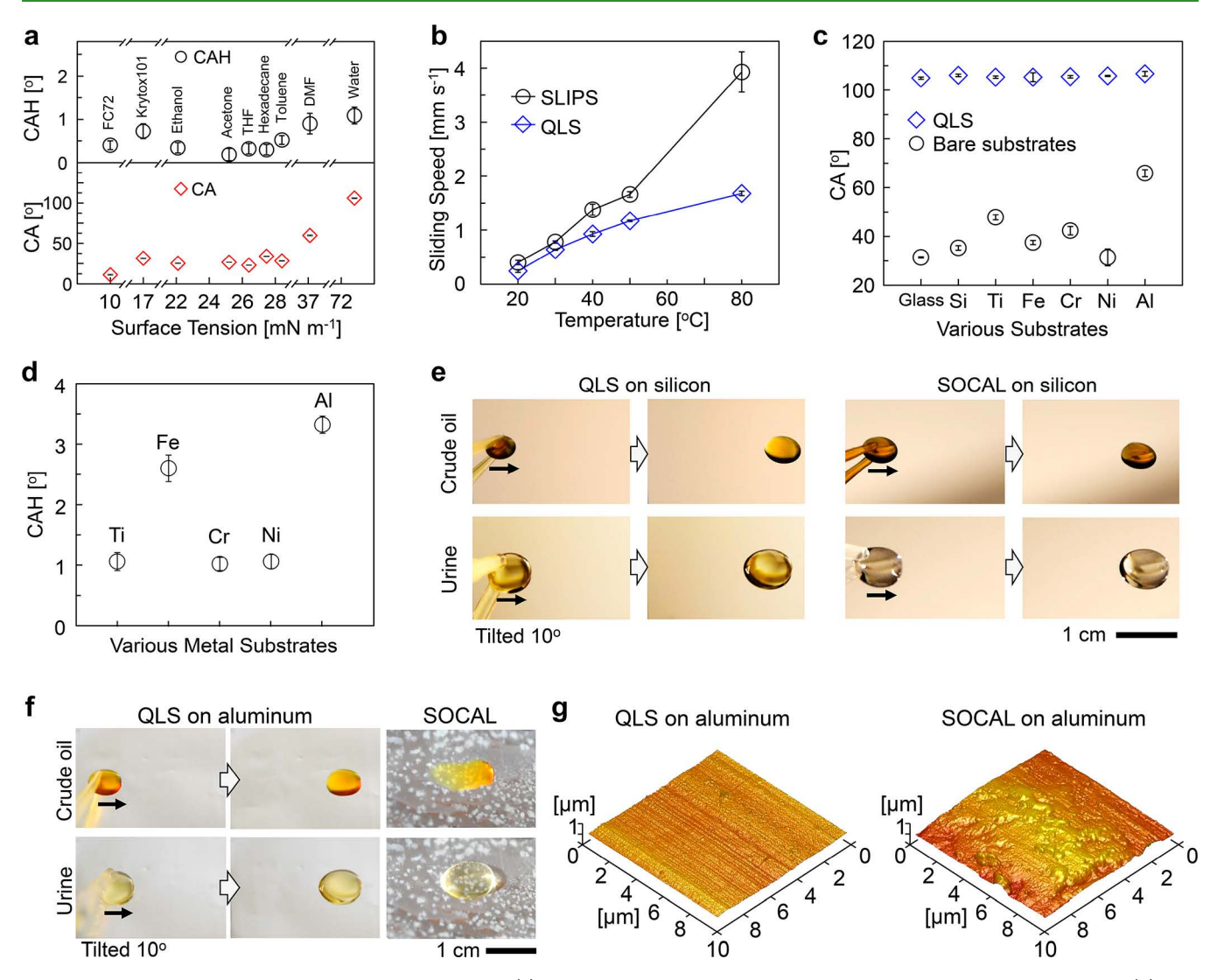


Figure 3. Liquid repellency of QLS on various substrates. (a) CAH and CA of various liquids on the QLS with a silicon substrate. (b) The temperature-dependent sliding speed of 5 μ L of hexadecane on the QLS with silicon substrate and SLIPS with Krytox101 lubricant at a tilt angle of 3°. The sliding speed values were averaged from 3 independent measurements. (c) CA of water on different substrates before and after coating with the QLS. (d) CAH of toluene on the QLS made on different metal substrates. (e) Liquid repellency of crude oil and urine on the QLS silicon vs SOCAL silicon. (f) Liquid repellency of crude oil and urine on the QLS aluminum foil vs SOCAL aluminum foil. These two liquids could slide on the QLS made on silicon and aluminum easily but get pinned on the SOCAL made on aluminum foil due to the corrosion spots on the surface. (g) 3D AFM images of QLS and SOCAL made on aluminum foil. The SOCAL on aluminum shows serious corrosion on the surface. The CAH and CA values in (a), (c), and (d) were averaged from at least 5 independent measurements by applying \sim 5 μ L droplets on the test platform.

temperature enables remarkably enhanced evaporation of liquid siloxane oligomer, providing a high interfacial concentration of reactant, as well as rapid hydrolysis and polycondensation (Figure S7). Therefore, the preparation of the samples at a higher temperature (T = 60 °C) can significantly increase the formation rate and the thickness of the polymer coating, resulting in an improved liquid repellency on the QLS. The QLS grafted within 10 to 720 min at 60 °C exhibits an ultralow CAH ($\Delta\theta$ < 1.8°), and the thickness of the polymer coating only slightly increases from 28.8 to 33.3 nm when the coating time varies from 10 to 720 min (Figure S8). It indicates that the equilibration for the growth of the polydimethylsiloxane polymer could be rapidly established in 10 min at 60 °C. After that, the polycondensation rate of the polymer on the surface is significantly inhibited by the accumulation of absorbed water that is generated from the reaction, even though reduced pressure is applied.³⁸ A slight increase of the SA from 4° to 6.5° was observed on the QLS when the grafting time was increased from 180 to 720 min due to less homogeneity of the coating at a longer coating time (Figure S6).

Overall, the ultralow CAH ($\Delta\theta=1.0^\circ$) of water droplets on the QLS at 60 °C for 60 min indicates the high mobility and nonentanglement of the grafted polymer with an optimized thickness of 30.1 nm. In comparison, a much larger CAH and SA were presented on the surface of cross-linked PDMS for water (CAH $\Delta\theta=11.4^\circ$, SA = 30°) and hexadecane (CAH $\Delta\theta=14.8^\circ$, SA = 23°) (Figure S9). This indicates that the flexible polymer of the QLS has been grafted in an orderly brush structure without cross-linking between tethered chains. The chemical composition of the QLS was analyzed by attenuated total reflection Fourier transform infrared spectroscopy (ATR-FTIR). As shown in Figure 2b, the characteristic peaks at 2965 cm⁻¹ (ν C–H), 1261 cm⁻¹ (ν Si–CH₃), 1039/1097 cm⁻¹ (ν

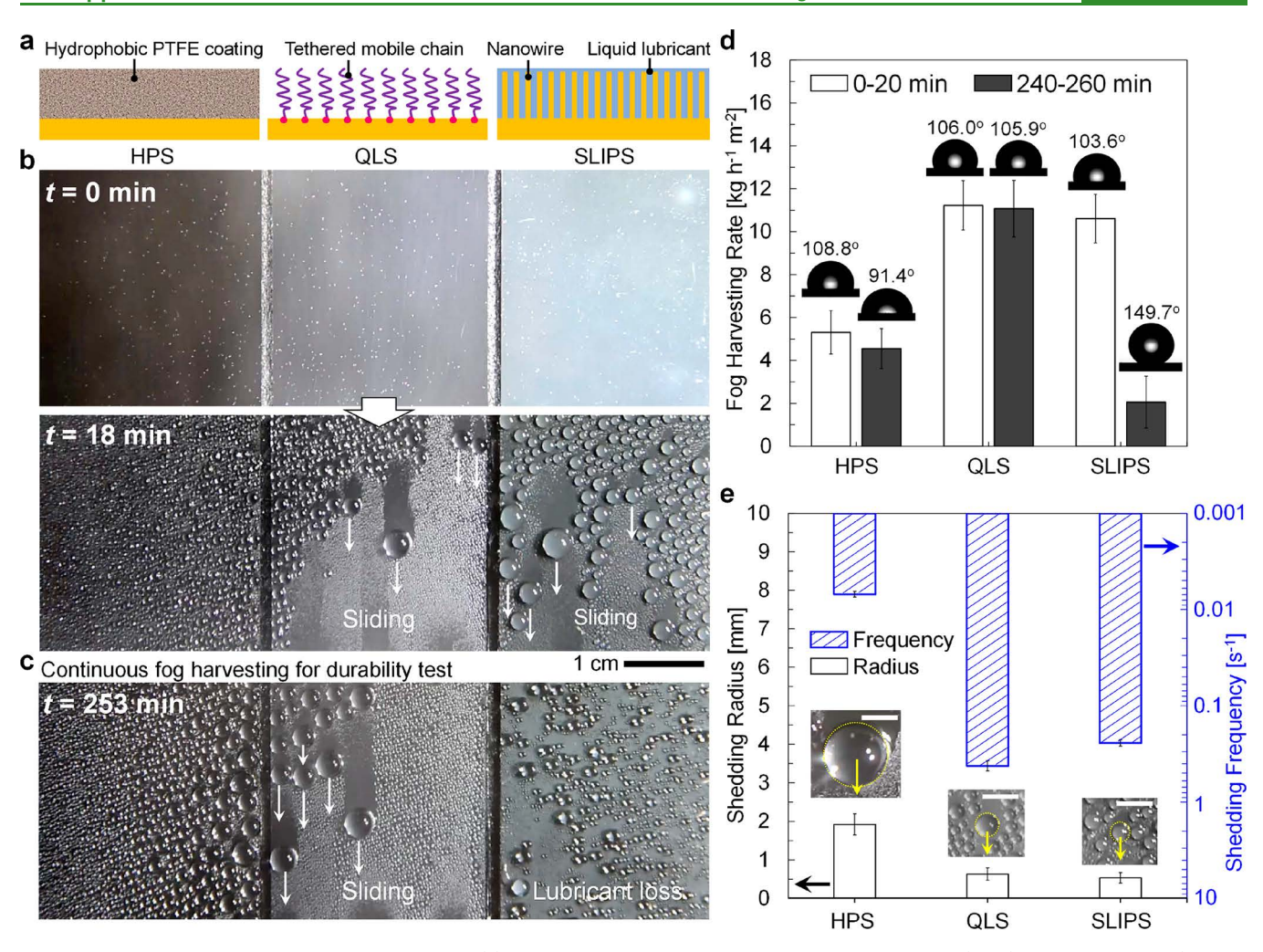


Figure 4. Performance of fog harvesting on the QLS. (a) Schematics of the PTFE-coated hydrophobic surface (HPS), QLS, and SLIPS (mineral oil-infused black silicon). (b) Comparison of fog harvesting on the three surfaces in 0–20 min. (c) Durable fog harvesting for 253 min without losing surface lubrication on QLS. (d) Fog harvesting rates on the HPS, QLS, and SLIPS. The insets present the water CA on different surfaces before and after the fog harvesting tests. The surfaces were positioned vertically during the fog harvesting tests by collecting water at 0–20 and 240–260 min during fog harvesting. (e) Variations of the average droplet shedding radius and shedding frequency on the HPS, QLS, and SLIPS at 0–20 min during fog harvesting. The insets show the images of shedding water droplets on the three surfaces for size comparison. All the fog harvesting data mentioned in (d) and (e) were averaged from at least 5 independent measurements. Scale bar: 2 mm.

Si–O–Si), and 806 cm⁻¹ (ν Si–(CH₃)₂) on the QLS indicate the successful grafting of flexible polymer, i.e., polydimethylsi-loxane. Compared with bare and plasma-treated silicon, the QLS displays enhanced absorption peaks at 3725 cm⁻¹ and 3000–3650 cm⁻¹, which correspond to the vibrations of Si–OH and O–H of adsorbed water molecules on the surface (inset in Figure 2b).

Repelling Liquids Regardless of Their Surface Tensions. The superior omniphobicity of the QLS with an ultralow CAH ($\Delta\theta \leq 1.0^{\circ}$) is applicable to a broad range of polar or nonpolar liquids with surface tensions from 10.0 to 72.8 mN m⁻¹ (Figure 3a and Table S4). Particularly, most of the organic liquids (e.g., toluene, hexadecane, acetone, Krytox101, and FC72) start to slide off on QLS at a tilted angle of less than 0.6° (Table S4). A sliding speed of 19.88 mm s⁻¹ of acetone (\sim 5 μ L) is achieved at a tilted angle of 10° (Figure S10 and Movie S2). Surprisingly, the highly wetting liquid such as FC72 with a surface tension of 10.0 mN m⁻¹ could also be rapidly repelled on the QLS even though the contact angle (CA) is around 11.2° (Figure S11). At an elevated temperature, the sliding speed of the hexadecane

droplets (5 μ L) on the tilted QLS (tilted angle 3°) is significantly increased from 0.24 mm s⁻¹ (20 °C) to 1.68 mm (80 °C) due to the reduced viscosity of the grafted polymer (Figures 3b and S12). The increased sliding speed was also observed on Krytox101 oil-infused black silicon (one type of SLIPS) at an elevated temperature (Movie S3). The result indicates that the grafted mobile chain can significantly enhance the performance of liquid repellency by increasing the surface temperature. 25,43 The nondefect and homogeneity of the polymer coating are critical for minimizing CAH. 27,3 QLS could be applied to various substrates, including glass, silicon, and aluminum. All of these substrates were hydrophilic before the QLS was coated, but the water CAs increased to ~105° on all of them after OLS was coated (Figures 3c and S13). It indicates that QLS was successfully made on those substrates and changed their surface wetting behaviors. Moreover, all QLS coated substrates show a small CAH ($\Delta heta$ < 4°) to toluene with a surface tension of 28.4 mN m⁻¹ (Figures 3d and S14).

We compared our QLS with the state-of-the-art liquid-like surface (i.e., SOCAL) on both silicon and aluminum

substrates. The QLS and SOCAL can both be coated on silicon and show superior repellency to crude oil and urine (Figure 3e and Movie S4), but the SOCAL cannot be coated on aluminum. The SOCAL was prepared with small molecule siloxane (Me₂Si(OMe)₂) with the molecular weight of 120 g/ mol as the grafting reagent.³⁷ The chlorine-terminated siloxane with a small molecular weight of 425-650 g/mol was used for comparison in the vapor phase according to previously published work in 1999.²² Due to the blocking of chain growth by the vast water generated in the reaction using small molecule siloxane, ^{22,29,44} only 4.0 nm of the polymer coating layer can be obtained on the SOCAL.³⁷ In addition, the SOCAL made on aluminum cannot repel any liquids and shows severe acid corrosion spots because of the sulfuric acid as the additive catalyst (Figure 3f,g, Movie S5, Figures S15 and S16). The grafting recipe from the prior work caused a high vapor concentration of hydrochloric acid during the hydrolysis and thus corroded the aluminum surface (Figures S15 and S16).32 As expected, the crude oil and urine spread on the bare substrates of silicon and aluminum leaving large wetted footprints (Figure S17). Our QLS is compatible with various substrates including aluminum because this grafting recipe can be proceeded without adding any external solvent or acid catalyst into the reaction system. In addition, the amount of corrosive hydrochloric acid generated during the reactions is largely reduced by using the siloxane oligomer with a high molecular weight as the grafting reagent. The QLS made on aluminum with excellent liquid repellency does not show any corrosion spots on the surface (Figures 3f,g, S15, and S16). The repellency of complex fluids shows the broad impacts of the newly developed surface. The QLS enabled repellency of crude oil on aluminum is important for petroleum transportation, while the rapid removal of urine is highly desirable to save water in toilets.

Sustainable Fog Harvesting and Self-Cleaning on the QLS. A surface with a hydrophobic property and small CAH is desired for the easy departure of captured droplets from the surface. Such a QLS with nonsticky performance to various liquids has a potential for long-term fog harvesting. As hydrophobic surfaces (HPSs) and liquid-infused surfaces have been extensively studied in fog harvesting, we compared the QLS (made on silicon) with the HPS (PTFE-coated silicon) and SLIPS (mineral oil-infused black silicon, one type of SLIPS) in fog harvesting (Figure 4a). The mineral oil was used as a control lubricant for the fabrication of the SLIPS because it could minimize the wrapping layer²⁰ and showed a better performance for water harvesting.⁴⁵ The CAs of water droplets on the HPS, QLS, and SLIPS were 108.8°, 106.0°, and 103.6°, respectively. This indicated their static wetting behaviors are close to each other. However, the water CAHs on the HPS, QLS, and SLIPS were 18.6°, 1.0°, and 1.1°, respectively (Figure S18). We firstly tested the fog harvesting continuously for 260 min. The QLS performed comparably to the SLIPS, while the HPS could not harvest water as efficiently due to the large CAH (Figure 4b). More importantly, after 4 h, the fog harvesting performance on the QLS remained as good as at the beginning, but on the SLIPS, most of the captured water droplets were pinned on the surface due to the depletion of liquid lubricant (Figure 4c and Movie S6). This clearly showed the exceptional durability of our QLS in long-term fog harvesting applications.

To quantify the fog harvesting rates on the three surfaces, we compared the fog harvesting rate at 0–20 and 240–260 min

(Figure 4d). QLS still exhibited an efficient fog harvesting rate of 11.07 kg h⁻¹ m⁻² after 260 min, which was close to that of 11.22 kg h⁻¹ m⁻² in the first 20 min (Figure 4d). There was a negligible change of water CA (from 106.0° to 105.9°) and CAH (from 1.0° to 1.2°) on the QLS, showing high stability in long-term fog harvesting (insets in Figures 4d and S18). However, the fog harvesting rate on the SLIPS decreased by 81% from 10.61 to 2.05 kg h^{-1} m⁻² (Figure 4d). The increased water CA from 103.6° to 149.7° illustrated the ability loss of the SLIPS due to the lubricant depletion along with the moving droplets (insets in Figure 4d). It is worth mentioning here that the sliding droplet on the SLIPS could not fully remove the lubricant that is penetrating inside the porous structures of black silicon. Thus, the air pocket inside the black silicon is randomly occupied by the lubricant molecules. The inhomogeneous surface chemistry of the SLIPS after long-term fog harvesting induces a high adhesion force to water droplets. Moreover, the surface will have jumping droplets, which are not as good as a sliding droplet for water collection in the fog harvesting process. As shown in Figure S18, the water CAH on the SLIPS increased largely from 1.1° to 38.6° after long-term fog harvesting, indicating a great lateral adhesion force (F_{LA}) to droplets on the surface. The CAH is the key criterion to reflect the lateral adhesion force of the droplet on a surface, as described by the Furmidge's relation in eq 1⁴⁶

$$F_{\rm LA} = w\gamma(\cos\theta_{\rm rec} - \cos\theta_{\rm adv}) \tag{1}$$

where w is the base contact width of the droplet with the surface and γ is the liquid surface tension. When the CAH $\Delta\theta$ is smaller, it is easier to remove the droplets from the surface (smaller $F_{1,A}$) and the sliding for the liquid repellency is better. As a comparison, the fog harvesting rate of the HPS (PTFEcoated surface, 5.4 kg h^{-1} m⁻²) in the first 20 min is ~53% lower than that of the QLS, indicating a comparatively slower rate for water harvesting (Figure 4d and Movie S6). Furthermore, we studied the droplet dynamics on those three surfaces (Figure 4e). The gravity-driven shedding characteristics of different surfaces were quantified by the average shedding radius/frequency⁴⁷ (Figure 4e). In the first 20 min, both the QLS and SLIPS presented low pinning to water droplets, displaying a small shedding radius of 0.61 and 0.52 mm because of the low water CAH, respectively (Figures 4b and S18 and Movie S6). The QLS showed a higher shedding frequency of 0.42 s⁻¹ than that of the SLIPS of 0.24 s⁻¹ (Figure 4e). The PTFE-coated surface displayed a large shedding radius and an extremely small shedding frequency due to a great lateral adhesion force on the surface (Figures 4e and \$18). Overall, during the long-term fog harvesting, the QLS could maintain the same performance as that at the beginning of the tests due to the durable lubrication provided from chemically bonded flexible polymer on the substrate.

Transparent and liquid-repellent surfaces are highly desired for solar panels, buildings, and cars due to their potential self-cleaning properties. As shown in Figure S19, the contaminant particles on the QLS could be completely taken away by water droplets without leaving any dust benefiting from the flexible polymer-mediated nanocoating (Movie S7). However, the superhydrophobic surface (SHS), SLIPS, and bare glass cannot be self-cleaned (Figure S20). Although a lot of research shows that the SHS could perform regular self-cleaning very well, it will fail in harsh conditions when the contaminant dust is stubborn and tiny enough to be embedded inside the surface structure of the SHS (Figure S19).

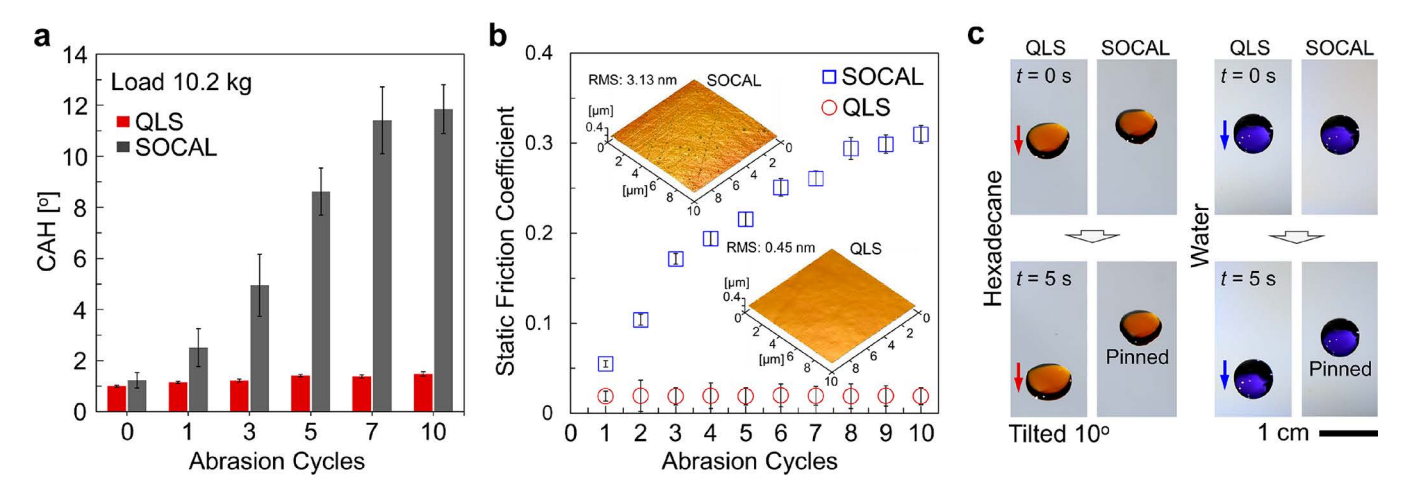


Figure 5. Comparison of liquid repellency on the QLS and SOCAL after harsh abrasion tests. (a) Comparison of water CAH on the QLS and SOCAL after 10 cycles of abrasion with a load of 10.2 kg. The CAH values were averaged from at least 5 independent measurements by applying \sim 5 μ L droplets on the test platform. (b) The static friction coefficient on the QLS and SOCAL, depending on the abrasion cycles with a load of 10.2 kg. The inset images show the 3D AFM images of the QLS and SOCAL after 10 cycles of abrasion. The roughnesses of the QLS and SOCAL are 0.45 nm and 3.13 nm, respectively. The static friction coefficient values were averaged from 3 independent measurements. (c) The repellency of 30 μ L of hexadecane (dyed in orange) and water (dyed in purple) on the QLS and SOCAL after 10 cycles of abrasion with a load of 10.2 kg, for which the QLS still shows superior liquid repellency. However, the droplets are pinned on the SOCAL. The QLS and SOCAL for the abrasion tests were made on silicon. A test load with tissue paper adhered to the bottom was applied to the surface for all abrasion tests.

Interfacial Durability of the QLS after Harsh Tests.

The QLS has the chemically bonded flexible polymer as a liquid-like lubricant on the flat surface, showing a low interfacial friction force, which exhibits the potential to address the long-standing durability issue of liquid-repellent surfaces. To elucidate this point, we compared the liquid repellency on the QLS with that on the SOCAL after harsh abrasion tests. We prepared the SOCAL coating on silicon with a drying time of 20 min at 21 °C according to a reported work.³⁷ The SOCAL surface showed a water CAH of 1.2°. When the reality application scenario of the liquid-repellent surfaces for windows, kitchenware, and medical apparatuses are considered, the mechanical abrasions are usually induced by wiping with tissue papers or textile fabric. Therefore, we used tissue paper as abrasion materials to do the test. In the abrasion test, a piece of tissue paper was in contact with the surfaces, and then, the load was added on the tissue paper for the abrasion test.6 Specifically, the water CAH on the QLS only had a negligible change from 1.0 to 1.4° after 10 cycles of abrasions with a load of 10.2 kg (load pressure of 144 kPa), while the CAH on the SOCAL sharply increased from 1.2 to 11.8° (Figures 5a and S21). When we changed the load from 10.2 to 5.9 kg (load pressure from 144 to 83 kPa), the water CAH on the SOCAL increased to 13.2° after 30 cycles while the water CAH on the QLS still showed 1.52° (Figure S22). It indicates that the antiwearing ability of the QLS is much better than that of the SOCAL. The main reason is that the thick layer of flexible polymer on the QLS can provide better lubrication to solids with an ultralow static friction coefficient of 0.019, which is 34.5% of that on SOCAL (Figure 1e). When the abrasion cycles were increased from 1 to 10, the static friction coefficient of the SOCAL increases greatly from 0.055 to 0.31, as the surface roughness increases from 0.26 to 3.13 nm, showing the failure of the coating (load of 10.2 kg, Figures 5b and \$23). In comparison, the QLS has a constant static friction coefficient of approximately 0.019 after the 10 cycles of abrasion tests. The surface roughness shows a negligible change from 0.35 to 0.45 nm, exhibiting durable lubrication

(Figures S2 and 5b). After 10 cycles of the severe abrasion test with a load of 10.2 kg, the QLS coated silicon still showed slippery characteristics to both water and hexadecane (Figure 5c, Movie S8). However, the SOCAL failed to repel any liquid after this severe abrasion test, reflecting a poor antiwearing ability.

Unlike the QLS, superomniphobic surfaces or liquid-infused surfaces rely on topographic textures to lock air or liquid lubricant for repelling water and oils. However, for those texture-mediated surfaces, mechanical occurrences such as a slight abrasion and scratches can lead to structural damage. With regard to the gentle abrasion and adhesion tests, the OLS could still repel water and hexadecane after 1000 cycles of those tests while the surface nanotextures of the SLIPS made of black silicon were damaged (Figures S24 and S25 and Movie S9). The lubrication layer of the flexible polymer on the QLS did not have an obvious morphology change after these tests demonstrated the robustness of the QLS (insets in Figure S25). The physical scratching enabled an increasing contact line pinning on the surface, leading to a large CAH.² However, both water and oil droplets could slide off the scratched QLS owing to the densely coated polymer layer on the surface (Figure S24 and Movie S9). Moreover, the QLS with continuous heating at 105 °C on a hot plate for more than 3 months showed unchanged surface morphology and exhibited liquid repellency toward water and hexadecane (Figure S26 and Movie S9). Overall, the superior durability of QLS has the potential to broaden the engineering applications for liquid-repellent surfaces.

Reduced Shear Strength for Ice Removal on the QLS. Ice formation and accretion cause inconvenience and even endanger human lives. For example, the accreted ice on wind turbine blades leads to a mass imbalance of the blades or even structural damage and reduces the power efficiency; the ice formed on aircrafts may lead to an inevitable loss of lift force and cause crash accidents. Consequently, passive strategies relying on surface engineering that reduce adhesion of ice are highly desired. The current state-of-the-art icephobic

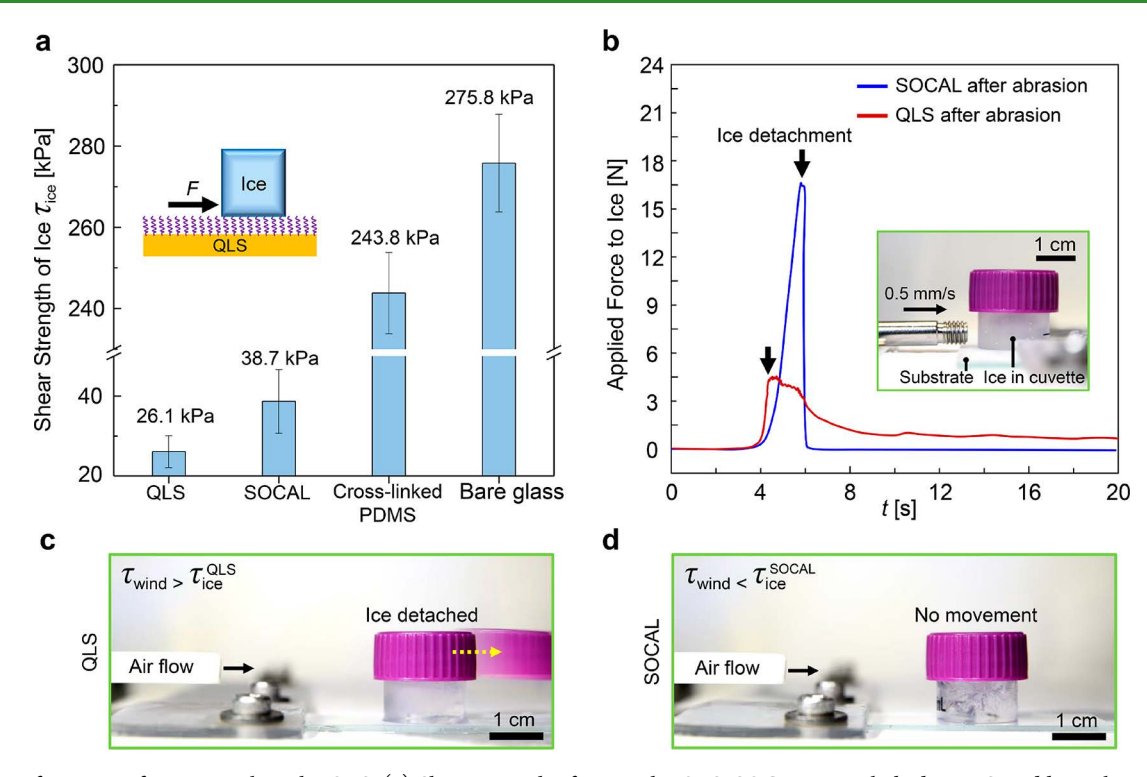


Figure 6. Performance of ice removal on the QLS. (a) Shear strength of ice on the QLS, SOCAL, cross-linked PDMS, and bare glass surface. The inset shows the schematic diagram for the tests. The shear strength of ice on various samples was averaged from 3 independent measurements. (b) The dynamic shear force of ice on the abraded QLS and SOCAL, which are abraded after 10 cycles with a load of 10.2 kg. The inset shows the test setup, where the test substrate with a cuvette containing ice was clamped and a force gauge was used to dislodge the bottom of the cuvette at a controlled speed of 0.5 mm/s. (c, d) The detachment of ice on the abraded QLS (c) and the abraded SOCAL (d) under the influence of wind (air flow). The ice easily detaches from the abraded QLS when wind is applied, but it shows no movement on the abraded SOCAL. Compressed air was used as the wind source. All the surfaces used for ice removal tests were made on glass instead of silicon because silicon wafers are thin and fragile.

technologies, such as liquid-infused surfaces, show dramatically reduced ice adhesion strength. Thowever, those surfaces suffer from severe durability challenges as the liquid lubricant will inevitably be depleted during ice removal. The QLS serves as persistent interfacial lubrication, which can transfer the ice/solid interface to an ice/quasi-liquid interface, providing not only robust liquid repellency but also a low interfacial shear strength to ice. To study the sustainability of the flexible polymer coating on the QLS for ice removal, we compared the shear strength of ice on the QLS before and after 10 cycles of severe abrasion with a load of 10.2 kg. The shear strength of ice (τ_{ice}) on a surface is calculated as

$$\tau_{\rm ice} = F_{\rm max}/A_{\rm ice} \tag{2}$$

where F_{max} is the maximum shear force that is required to remove adhered ice from the surface in the lateral direction and A_{ice} is the contact area between the ice and the surface. Herein, the QLS has the chemically bonded flexible polymer as a liquid-like lubricant on the flat surface. Thus, it can effectively and sustainably reduce the adhesion force between the ice and substrate. The shear strength of ice on the QLS is as low as 26.1 kPa, which is 67.4%, 10.7%, and 9.5% of that on the newly fabricated SOCAL (38.7 kPa), cross-linked PDMS (243.8 kPa), and bare glass surface (275.8 kPa), respectively (Figure 6a). After 10 cycles of abrasions with a load of 10.2 kg, the QLS still shows a steadily low shear strength of ice of 29.4 kPa (Figure S27), which demonstrates the robustness of the QLS for ice removal. In comparison, the shear strength of ice on the SOCAL increases dramatically from 38.7 to 103.2 kPa due to the failure of the surface coating, i.e., an increase of 166.7%

(Figures 6a, S23, and S27). Figure 6b shows the dynamic shear forces of ice on the QLS and SOCAL after abrasions. According to the standard ice adhesion test, ⁵¹ a setup consisting of a force gauge and a Peltier plate was used to measure the shear strength of ice on the surfaces (inset in Figure 6b). The probe of the force gauge dislodged the bottom of the ice at a controlled speed of 0.5 mm/s, and the ice was detached from the surfaces when the shear force increased to the maximum value of 4.4 N on the QLS and 16.7 N on the SOCAL, respectively (Figure 6b and Movie S10). It demonstrates that the QLS with the thicker flexible polymer coating can significantly reduce the interfacial shear strength and provides sustainable quasi-liquid lubrication for ice

In practical applications, the accreted ice on the exposed surfaces such as wind turbine blades, aircrafts, or vehicles usually shed off from the surface under natural forces provided by wind, gravity, or vibration. To evaluate the practical ice removal performance of the QLS, we designed the test for wind-assisted ice removal. Compressed air was used as the wind source, and a flow meter was equipped for the measurement of the wind pressure acting on the ice (Figure S28). The system could provide a stable wind pressure of \sim 4.6 kPa during the whole testing time of 60 s (Figure S28). We abraded the QLS and SOCAL for 10 cycles with a load of 10.2 kg and tested those abraded surfaces for ice removal. Figure 6c shows that the ice on the abraded QLS could be rapidly detached from the surface in 2 s when the wind shear strength was applied (Movie S11). However, the ice adhered firmly on the SOCAL and showed no movement due to the high shear strength of ice (103.2 kPa) on the SOCAL (Figures 6b,d and S27). The results showed that the QLS enables both liquid repellency and ice removal in harsh conditions. This is the first study to show that the flexible polymer-grafted surface significantly reduces the shear strength of ice. We envision that the robust QLS with a low shear strength of ice can enable the design of the next generation durable anti-/de-icing materials, which can potentially be applied to wind turbine blades, aircraft, and power lines.

CONCLUSIONS

We have successfully developed a quasi-liquid surface with tethered flexible polymers for sustainable liquid repellency, fog harvesting, and ice removal. Such a surface could be made on various substrates such as silicon, glass, and aluminum and achieve a polymer thickness as thick as 30.1 nm. The mobile chains of the flexible polymers grafted on the QLS provide superior interfacial lubrication to both liquids and solids. The QLS can repel diverse liquids from water to ultralow surface tension liquids (e.g., FC72 and Krytox101) and complex fluids (e.g., crude oil and urine). The QLS exhibited an impressive durability in fog harvesting compared with mineral oil-infused surfaces, as droplet shedding could not deplete the tethered polymer coating. Although the state-of-the-art liquid-like surface (i.e., SOCAL) was damaged by harsh abrasions, the QLS was able to survive and maintain its robust performace for liquid repellency and ice removal. In addition to the demonstrations in this work, we envision that the QLS may pave a way for potential applications, such as drag reduction, antifouling, dropwise condensation, and water harvesting.

■ METHODS

Fabrication of the Quasi-Liquid Surface on Various Substrates. The quasi-liquid surface was made by tethering the flexible polymer of polydimethylsiloxane (PDMS) on a solid substrate with a one-step self-catalyzed grafting method. Specifically, the oxygen plasma-treated substrates were placed upside down on the cover of a petri dish. Then, the petri dish (size: diameter, 150 mm; height, 15 mm) containing 800 µL of liquid chlorine-terminated siloxane oligomer was placed in a vacuum oven (0.15 Torr) at 60 °C for 60 min. The liquid was dispersed uniformly on the surface of the petri dish by gently swinging the petri dish before placing it into the vacuum oven. This one-step vapor phase method (i.e., no direct contact between the substrates and liquid reagent) could graft flexible polymer on the solid substrates. Sequentially, the substrates were rinsed with abundant isopropyl alcohol (IPA), toluene, acetone, and water, successively. Note that the liquid phase reaction (i.e., substrates are contacted with liquid reagent) could also be applied for successful grafting. All QLS samples, unless otherwise specified, were prepared in the vapor phase at 60 °C for 60 min.

Contact Angle Measurements. The contact angle measurements were carried out using a standard goniometer (Model 290, Ramé-hart) at room temperature under ambient conditions (20–22 °C, ~40% relative humidity). All the contact angle values were averaged from at least 5 independent measurements by applying ~5 μ L droplets on the test platform. For the measurement of contact angle hysteresis, the surface was tilted with respect to the horizontal plane until the liquid droplet started to slide along the surface. Then, advancing, receding, and sliding angles of the droplet were calculated by a computer program (Ramé-hart DROPimage Advanced) in which the drops were fitted into a spherical cap.

Fog Harvesting and Self-Cleaning Tests. To make a better comparison study for fog harvesting, the hydrophobic surface (HPS,PTFE-coated silicon), mineral oil-infused black silicon (SLIPS), and QLS (made on silicon), which has the same size of 1.4 mm × 3.3 mm, were vertically immobilized at the same height. A

commercial ultrasonic humidifier (EE-5301, Crane) was used to produce mist. The fog flow was directed to the vertically hanged surfaces at an angle of $45^{\circ} \pm 5^{\circ}$, and the distance between the mist outlet to the vertical substrates was ~ 20 cm. Images of the absorbed water droplet could be obtained from the snapshots of the videos recorded using a digital single-lens reflex camera (D5600, Nikon) equipped with a zoom lens (AF Zoom-NIKKOR 24-85 mm f/2.8-4D IF Lens, Nikon). We can get the projections of the droplets, i.e., the width of the droplet (w), from the recorded images. We assume that the absorbed water droplet could be approximately fitted into the spherical cap; therefore, the shedding radius (R) of the water droplet, i.e., the base contact radius of the droplet with the surface, can be calculated as R = w/2. The shedding frequency (f) of the water droplets was obtained by counting the number (N) of droplets that slid on the surface in a surface area of 7.5 cm² (3 cm \times 2.5 cm) over a period of time (t), which can be described as f = N/t. A clean beaker was placed under the drainage outlet of the substrate to collect the dripping water. The water collection was started after the first droplet slid off the surface. Then, the weight of the beaker before (m_0) and after (m_1) the water collection time (t) was measured by an analytical balance. The average fog harvesting rate could be calculated as $(m_1$ m_0)/(t × A), where A is the surface area of the substrate and t is 5 min. All the fog harvesting data mentioned above was averaged from at least 5 independent measurements. To have better visibility in the self-cleaning test, the transparent glass substrates were used, in which a superhydrophobic glass (NeverWet coating), the SLIPS (crosslinked PDMS infused with silicone oil), and a clean glass slide were used as the comparison substrates for the QLS (made on glass). The iron oxide powder with a particle size of less than 5 μ m was used as the "contaminant". A similar amount of iron powder was sprinkled on different substrates and then was slightly pressed to imitate stubborn contaminant dust; next, the substrates (with a tilted angle of 30°) were washed with continuous water drops. The digital camera was used to record the whole self-cleaning process.

Durability Tests. For the high-temperature aging test, the QLS sample was placed on a hot plate (PC-400D, Corning) for which the temperature was set as 105 °C. At set intervals, the samples were taken off the hot plate for testing of water CAH. For the long aging period, the sample was covered with glass petri dish to avoid the dust contamination. For the comparison of the QLS and SLIPS on the abrasion test, a piece of tissue paper adhered to the bottom of a 200 g weight (contact diameter of the weight with the surface is 3 cm). Then, the load was placed on the surface, and the abrasion movement proceeded with a pulling speed of ~ 0.12 m/s in the abrasion test. To do the severe abrasion test on the surface of the QLS and SOCAL, 10.2 and 5.9 kg loads with tissue paper adhered to the bottom were applied to the surface, respectively (contact diameter of the weight with the surface was 3 cm). The force required to dislodge the load was recorded using a force gauge (Nextech DFS500) at a controlled speed of 0.5 mm/s. For the comparison of the QLS and SLIPS on the adhesion test, a piece of double-sided adhesive tape (2.5 cm \times 2.5 cm) was adhered to the bottom of a 200 g weight and, then, the load was placed on the surface for the adhesion test. After each specific abrasion or adhesion cycle, the water CAH was tested on the surface by a goniometer.

Ice Removal Tests. The ice removal tests were carried out under ambient conditions (20–22 °C, ~40% relative humidity). We took 3 independent measurements of shear force to calculate the shear strength of ice on various samples. Note that all the samples used for ice removal tests were made on glass. A plastic cuvette (height: 2.1 cm; inner diameter at the bottom: 1.4 cm; Figure S29) containing deionized water (2 mL) was placed on the top of the samples. Then, we put it inside the refrigerator overnight to ensure the water completely froze. We built up a testing platform consisting of a force gauge (Nextech DFS500) integrated on a syringe pump (PHD 2000, Harvard Apparatus) and a Peltier plate (CP-200HT-TT, TE Technology, Inc.), where the screw of the syringe pump can provide the precise movement for the force gauge, thus controlling the pushing or pulling speed. The probe of the force gauge could push at the very bottom of the cuvette near the base of the substrate driven by

the syringe pump at a controlled speed of 0.5 mm/s. The shear force was continuously recorded by the force gauge software (NexGraph). For wind-assisted ice removal, we used an airflow meter (Digi-Sense 20250-13) to measure the wind pressure of the flow of air (Figure S28). We set the temperature of the Peltier plate as $-10~^{\circ}\text{C}$ to avoid the melting of the ice during all the tests.

Characterization. All the substrates were treated in an oxygen plasma cleaner (PX-250, March Asher) for 20 min at 200 W with 200 mTorr O₂ gas before grafting. The optical transparency of these surfaces was studied using a PerkinElmer Lambda 900 UV-vis/NIR spectrophotometer with a wavelength range from 200 to 900 nm at a resolution of 1 nm. An FT-IR/ATR spectrometer (Nexus 4700, Nicolet) was employed to study the chemical compositions of the surfaces before and after grafting with the PDMS polymer. Atomic force microscopy (AFM) measurements were carried out in tapping mode using a Nanoscope V controller on a multimode microscope (Multimode IV, Bruker). The cross-section morphology of the QLS on silicon was characterized by the scanning electron microscope (SEM, Supra-40, Zeiss). The Sentech 800 ellipsometer was used to analyze the thickness of the grafted PDMS polymer on the QLS at an incident angle of 70° and with a He–Ne laser as the light source (λ = 632.8 nm). The Cauchy model was used to calculate the thickness, in which the thickness of the SiO₂ layer on the oxygen plasma-treated silicon was used as the baseline layer. The average thickness was obtained by 5 independent measurements at different positions on the

ASSOCIATED CONTENT

Solution Supporting Information

The Supporting Information is available free of charge at https://pubs.acs.org/doi/10.1021/acsami.0c02014.

Discussions regarding the chemical materials, preparation, and characterization of the quasi-liquid surface; comparison of liquid repellency for the quasi-liquid surface fabricated in this work and other omniphobic surfaces; surfaces prepared from chlorine-terminated siloxane oligomer; comparison of the contact angle, contact angle hysteresis, and the sliding angle; schematic for the preparation of the QLS; AFM and SEM images of the surfaces before and after QLS coating; UV-vis spectra; comparison of friction coefficients; sliding angles; schematics showing the influence of temperature on the evaporation of chlorine-terminated siloxane oligomer; θ_{Adv} , θ_{Rec} , and CAH of water droplets on the QLS and the corresponding thickness of the flexible polymer; contact angle, contact angle hysteresis, and sliding angle for water and hexadecane; time-sequence images and sliding speeds of different liquids on QLS; images of water and contact angles; comparisons of the recipe proposed in this work and previously reported recipes for grafting flexible polymer of PDMS on the aluminum foil; liquid repellency of crude oil and urine; water CAH of the PTFE-coated hydrophobic surface, QLS, and SLIPS before and after the fog harvesting test; self-cleaning on the QLS and SHS; performance of the SLIPS and bare glass slides used for self-cleaning; apparatus of the abrasion test; comparison of water CAH on the QLS and SOCAL; AFM images of the SOCAL made on silicon; durable liquid repellency of water and organic liquids in harsh conditions; images showing the surface of the SLIPS; schematic and digital photos of high-temperature aging test and liquid repellency of the QLS to water and hexadecane; shear strength of ice on the QLS and SOCAL; wind pressure

induced by the compressed air; side cross-section view of the cuvette (PDF)

Liquid repellency of the quasi-liquid surface to water and highly wetting Krytox101 oil (MP4)

Sliding speed of various liquids on the quasi-liquid surface (MP4)

Sliding speed of hexadecane on the quasi-liquid surface and the liquid-infused surface at different temperatures (MP4)

Quasi-liquid surface made on either silicon or aluminum repelling different liquids even for complex fluids of crude oil and urine (MP4)

Comparison of liquid repellency on the quasi-liquid surface, the SOCAL, and small molecule siloxane-grafted surface (MP4)

Fog harvesting performance of the quasi-liquid surface (MP4)

Self-cleaning performance of the quasi-liquid surface (MP4)

Liquid repellency of the quasi-liquid surface and SOCAL to water and hexadecane after abrasion test (MP4)

Durable liquid repellency of the quasi-liquid surface and SLIPS to water and oil after harsh tests (MP4)

Ice removal test on the quasi-liquid surface and the SOCAL (MP4)

Wind-assisted ice removal on the quasi-liquid surface and the SOCAL (MP4)

■ AUTHOR INFORMATION

Corresponding Author

Xianming Dai — Department of Mechanical Engineering, The University of Texas at Dallas, Richardson, Texas 75080, United States; orcid.org/0000-0001-5050-2867; Email: Dai@utdallas.edu

Authors

Lei Zhang — Department of Mechanical Engineering, The University of Texas at Dallas, Richardson, Texas 75080, United States; o orcid.org/0000-0003-4975-6821

Zongqi Guo – Department of Mechanical Engineering, The University of Texas at Dallas, Richardson, Texas 75080, United States

Jyotirmoy Sarma — Department of Mechanical Engineering, The University of Texas at Dallas, Richardson, Texas 75080, United States

Complete contact information is available at: https://pubs.acs.org/10.1021/acsami.0c02014

Author Contributions

L.Z. and X.D. conceived the research. X.D. supervised the research. L.Z. and X.D. designed the experiments. L.Z. and Z.G. carried out the liquid repellency and fog harvesting studies. L.Z. and J.S. performed the ice removal studies. All authors discussed the results, conducted the data analysis, and wrote the manuscript.

Notes

The authors declare the following competing financial interest(s): The authors declare that a United States provisional patent has been filed for this work.

ACKNOWLEDGMENTS

The authors gratefully acknowledge the startup funding support (Grant No. 40030467) by the University of Texas at Dallas (UT Dallas), National Science Foundation (NSF) in the United States (Award No. 1929677), and the Young Investigator Program at Army Research Office (Award No. W911NF1910416). This project was partially funded by the Office of Research at UT Dallas through the Core Facility Voucher Program. The authors are grateful to Rong Wang for her help on the preparation of the metal-deposited silicon wafers. We also thank Prof. Zuankai Wang for suggesting the terminology of "quasi-liquid".

REFERENCES

- (1) Wong, T.-S.; Kang, S. H.; Tang, S. K.; Smythe, E. J.; Hatton, B. D.; Grinthal, A.; Aizenberg, J. Bioinspired Self-Repairing Slippery Surfaces with Pressure-Stable Omniphobicity. *Nature* **2011**, 477, 443–447.
- (2) Deng, X.; Mammen, L.; Butt, H.-J.; Vollmer, D. Candle Soot as a Template for a Transparent Robust Superamphiphobic Coating. *Science* **2012**, 335, 67–70.
- (3) Tuteja, A.; Choi, W.; Ma, M.; Mabry, J. M.; Mazzella, S. A.; Rutledge, G. C.; McKinley, G. H.; Cohen, R. E. Designing Superoleophobic Surfaces. *Science* **2007**, *318*, 1618–1622.
- (4) Liu, T.; Kim, C.-J. Turning a Surface Superrepellent even to Completely Wetting Liquids. *Science* **2014**, *346*, 1096–1100.
- (5) Dai, X.; Sun, N.; Nielsen, S. O.; Stogin, B. B.; Wang, J.; Yang, S.; Wong, T.-S. Hydrophilic Directional Slippery Rough Surfaces for Water Harvesting. Sci. Adv. 2018, 4, eaaq0919–0928.
- (6) Lu, Y.; Sathasivam, S.; Song, J.; Crick, C. R.; Carmalt, C. J.; Parkin, I. P. Robust Self-Cleaning Surfaces That Function When Exposed to Either Air or Oil. *Science* **2015**, 347, 1132–1135.
- (7) Pan, S.; Kota, A. K.; Mabry, J. M.; Tuteja, A. Superomniphobic Surfaces for Effective Chemical Shielding. *J. Am. Chem. Soc.* **2013**, 135, 578–581.
- (8) Kreder, M. J.; Alvarenga, J.; Kim, P.; Aizenberg, J. Design of Anti-Icing Surfaces: Smooth, Textured or Slippery? *Nat. Rev. Mater.* **2016**, *1*, 15003–15017.
- (9) Bonn, D.; Eggers, J.; Indekeu, J.; Meunier, J.; Rolley, E. Wetting and Spreading. *Rev. Mod. Phys.* **2009**, *81*, 739–805.
- (10) Dai, X.; Stogin, B. B.; Yang, S.; Wong, T.-S. Slippery Wenzel State. ACS Nano **2015**, *9*, 9260–9267.
- (11) Cassie, A. B. D.; Baxter, S. Wettability of Porous Surfaces. *Trans. Faraday Soc.* **1944**, *40*, 546–550.
- (12) Wenzel, R. N. Resistance of Solid Surfaces to Wetting by Water. *Ind. Eng. Chem.* **1936**, 28, 988–994.
- (13) Lafuma, A.; Quéré, D. Slippery Pre-Suffused Surfaces. Europhys. Lett. 2011, 96, 56001-56004.
- (14) Kim, P.; Wong, T.-S.; Alvarenga, J.; Kreder, M. J.; Adorno-Martinez, W. E.; Aizenberg, J. Liquid-Infused Nanostructured Surfaces with Extreme Anti-Ice and Anti-Frost Performance. ACS Nano 2012, 6, 6569–6577.
- (15) Nosonovsky, M.; Hejazi, V. Why Superhydrophobic Surfaces Are Not Always Icephobic. ACS Nano 2012, 6, 8488–8491.
- (16) Miljkovic, N.; Enright, R.; Nam, Y.; Lopez, K.; Dou, N.; Sack, J.; Wang, E. N. Jumping-Droplet-Enhanced Condensation on Scalable Superhydrophobic Nanostructured Surfaces. *Nano Lett.* **2013**, *13*, 179–187.
- (17) Rosenberg, B. J.; Van Buren, T.; Fu, M. K.; Smits, A. J. Turbulent Drag Reduction over Air-and Liquid-Impregnated Surfaces. *Phys. Fluids* **2016**, *28*, 015103–015110.
- (18) Maynes, D.; Webb, B. W.; Davies, J. Thermal Transport in a Microchannel Exhibiting Ultrahydrophobic Microribs Maintained at Constant Temperature. *J. Heat Transfer* **2008**, *130*, 022402–022408.
- (19) Preston, D. J.; Song, Y.; Lu, Z.; Antao, D. S.; Wang, E. N. Design of Lubricant Infused Surfaces. ACS Appl. Mater. Interfaces 2017, 9, 42383–42392.

- (20) Schellenberger, F.; Xie, J.; Encinas, N.; Hardy, A.; Klapper, M.; Papadopoulos, P.; Butt, H.-J.; Vollmer, D. Direct Observation of Drops on Slippery Lubricant-Infused Surfaces. *Soft Matter* **2015**, *11*, 7617–7626.
- (21) Lv, J.; Song, Y.; Jiang, L.; Wang, J. Bio-Inspired Strategies for Anti-Icing. ACS Nano 2014, 8, 3152-3169.
- (22) Chen, W.; Fadeev, A. Y.; Hsieh, M. C.; Öner, D.; Youngblood, J.; McCarthy, T. J. Ultrahydrophobic and Ultralyophobic Surfaces: Some Comments and Examples. *Langmuir* **1999**, *15*, 3395–3399.
- (23) Krumpfer, J. W.; McCarthy, T. J. Rediscovering Silicones: "Unreactive" Silicones React With Inorganic Surfaces. *Langmuir* **2011**, 27, 11514–11519.
- (24) Cheng, D. F.; Urata, C.; Masheder, B.; Hozumi, A. A Physical Approach to Specifically Improve the Mobility of Alkane Liquid Drops. J. Am. Chem. Soc. 2012, 134, 10191–10199.
- (25) Cheng, D. F.; Urata, C.; Yagihashi, M.; Hozumi, A. A Statically Oleophilic but Dynamically Oleophobic Smooth Nonperfluorinated Surface. *Angew. Chem.* **2012**, *124*, 3010–3013.
- (26) Hu, H.; Liu, G.; Wang, J. Clear and Durable Epoxy Coatings that Exhibit Dynamic Omniphobicity. *Adv. Mater. Interfaces* **2016**, 3, 1600001–1600006.
- (27) Wooh, S.; Vollmer, D. Silicone Brushes: Omniphobic Surfaces with Low Sliding Angles. *Angew. Chem., Int. Ed.* **2016**, *55*, 6822–6824.
- (28) Yu, L.; Chen, G. Y.; Xu, H.; Liu, X. Substrate-Independent, Transparent Oil-Repellent Coatings with Self-Healing and Persistent Easy-Sliding Oil Repellency. *ACS Nano* **2016**, *10*, 1076–1085.
- (29) Flagg, D. H.; McCarthy, T. J. Rapid and Clean Covalent Attachment of Methylsiloxane Polymers and Oligomers to Silica Using B (C6F5) 3 Catalysis. *Langmuir* **2017**, *33*, 8129–8139.
- (30) Liu, P.; Zhang, H.; He, W.; Li, H.; Jiang, J.; Liu, M.; Sun, H.; He, M.; Cui, J.; Jiang, L.; Yao, X. Development of "Liquid-Like" Copolymer Nanocoatings for Reactive Oil-Repellent Surface. *ACS Nano* **2017**, *11*, 2248–2256.
- (31) Boban, M.; Golovin, K.; Tobelmann, B.; Gupte, O.; Mabry, J. M.; Tuteja, A. Smooth, All-Solid, Low-Hysteresis, Omniphobic Surfaces with Enhanced Mechanical Durability. *ACS Appl. Mater. Interfaces* **2018**, *10*, 11406–11413.
- (32) Singh, N.; Kakiuchida, H.; Sato, T.; Hönes, R.; Yagihashi, M.; Urata, C.; Hozumi, A. Omniphobic Metal Surfaces with Low Contact Angle Hysteresis and Tilt Angles. *Langmuir* **2018**, *34*, 11405–11413.
- (33) Zhang, G.; Liang, B.; Zhong, Z.; Huang, Y.; Su, Z. One-Step Solvent-Free Strategy for Covalently Attached, Substrate-Independent Transparent Slippery Coating. *Adv. Mater. Interfaces* **2018**, *5*, 1800646–1800652.
- (34) Zhong, X.; Hu, H.; Yang, L.; Sheng, J.; Fu, H. Robust Hyper-Branched Polyester-Based Anti-Smudge Coatings for Self-cleaning, Anti-graffiti and Chemical Shielding. *ACS Appl. Mater. Interfaces* **2019**, *11*, 14305–14312.
- (35) Wooh, S.; Butt, H. J. A Photocatalytically Active Lubricant-Impregnated Surface. *Angew. Chem., Int. Ed.* **2017**, *56*, 4965–4969.
- (36) Wooh, S.; Encinas, N.; Vollmer, D.; Butt, H. J. Stable Hydrophobic Metal-Oxide Photocatalysts via Grafting Polydimethylsiloxane Brush. *Adv. Mater.* **2017**, *29*, 1604637–1604643.
- (37) Wang, L.; McCarthy, T. J. Covalently Attached Liquids: Instant Omniphobic Surfaces with Unprecedented Repellency. *Angew. Chem., Int. Ed.* **2016**, *55*, 244–244.
- (38) Herzberg, W. J.; Marian, J. E.; Vermeulen, T. The Receding Contact Angle. J. Colloid Interface Sci. 1970, 33, 164–171.
- (39) Kuniyoshi, M.; Takahashi, M.; Tokuda, Y.; Yoko, T. Hydrolysis and Polycondensation of Acid-Catalyzed Phenyltriethoxysilane (PhTES). *J. Sol-Gel Sci. Technol.* **2006**, *39*, 175–183.
- (40) Jones, R. A. Amorphous Materials: Glasses with Liquid-Like Surfaces. *Nat. Mater.* **2003**, *2*, 645–646.
- (41) Bodas, D.; Khan-Malek, C. Formation of More Stable Hydrophilic Surfaces of PDMS by Plasma and Chemical Treatments. *Microelectron. Eng.* **2006**, 83, 1277–1279.
- (42) Mahmoudi, M.; Javaherian Naghash, H. Synthesis and Characterization of a Novel Hydroxyl-Terminated Polydimethylsilox-

- ane for Application in the Silicone-Modified Acrylic-Grafted Polyester Resins. J. Adhes. Sci. Technol. 2015, 29, 1341–1359.
- (43) Luap, C.; Goedel, W. A. Linear Viscoelastic Behavior of End-Tethered Polymer Monolayers at the Air/Water Interface. *Macromolecules* **2001**, *34*, 1343–1351.
- (44) Fadeev, A. Y.; McCarthy, T. J. Self-Assembly Is Not the Only Reaction possible Between Alkyltrichlorosilanes and Surfaces: Monomolecular and Oligomeric Covalently Attached Layers of Dichloro-and Trichloroalkylsilanes on Silicon. *Langmuir* **2000**, *16*, 7268–7274.
- (45) Park, K.-C.; Kim, P.; Grinthal, A.; He, N.; Fox, D.; Weaver, J. C.; Aizenberg, J. Condensation on Slippery Asymmetric Bumps. *Nature* **2016**, *531*, 78–84.
- (46) Furmidge, C. Studies at Phase Interfaces. I. The Sliding of Liquid Drops on Solid Surfaces and a Theory for Spray Retention. *J. Colloid Sci.* **1962**, *17*, 309–324.
- (47) Baratian, D.; Dey, R.; Hoek, H.; Van Den Ende, D.; Mugele, F. Breath Figures Under Electrowetting: Electrically Controlled Evolution of Drop Condensation Patterns. *Phys. Rev. Lett.* **2018**, 120, 214502—214506.
- (48) Geyer, F.; D'Acunzi, M.; Sharifi-Aghili, A.; Saal, A.; Gao, N.; Kaltbeitzel, A.; Sloot, T.-F.; Berger, R.; Butt, H.-J.; Vollmer, D. When and How Self-Cleaning of Superhydrophobic Surfaces Works. *Sci. Adv.* **2020**, *6*, eaaw9727–9737.
- (49) Golovin, K.; Dhyani, A.; Thouless, M.; Tuteja, A. Low-Interfacial Toughness Materials for Effective Large-Scale Deicing. *Science* **2019**, 364, 371–375.
- (50) Beemer, D. L.; Wang, W.; Kota, A. K. Durable Gels with Ultra-Low Adhesion to Ice. J. Mater. Chem. A 2016, 4, 18253–18258.
- (51) Rønneberg, S.; He, J.; Zhang, Z. The Need for Standards in Low Ice Adhesion Surface Research: a Critical Review. *J. Adhes. Sci. Technol.* **2020**, *34*, 319–347.